Acta Cryst. (1993). B49, 19–28

Structure and Twinning of $RbLiCrO_4$ Crystals

BY I. P. MAKAROVA AND I. A. VERIN

Institute of Crystallography, Academy of Sciences, Leninsky pr. 59, 117333 *Moscow, Russia*

AND K. S. ALEKSANDROV

Institute of Physics, Siberian Division of the Academy of Sciences, 660036 *Krasnoyarsk, Russia*

(*Received* 16 *January* 1992; *accepted* 5 *June* 1992)

Abstract

The crystal structures of the G_3 (space group $P31c$) and G_2 (space group $P6_3$) phases of $RbLiCrO_4$ have been determined from X-ray diffraction data (Mo $K\alpha$ radiation) at 293, 428, 493 and 523 K (G_3 phase) and 553 and 583 K (G_2 phase). The $RbLiCrO_4$ crystals exhibit twinning by merohedry with twin laws in the G_3 phase: $2 \parallel [001]$, $m \perp [001]$, $\bar{1}$; in the G_2 phase: $m \parallel [001]$, $2 \perp [001]$, $\bar{1}$. The analysis of diffraction intensities and influence of anomalous scattering on them provided the unambiguous determination of the twin laws for all the specimens investigated. The structure has been refined using the approximation of the anharmonic thermal vibrations of atoms.

Introduction

First studies of phase transitions in $RbLiCrO_4$ crystals were reported by Kruglik, Mel'nikova, Aleksandrov & Grankina (1990) and Kruglik, Mel'nikova, Tolochko, Makarova & Aleksandrov (1991). Investigation of $RbLiCrO_4$ by differential thermal analysis, optical observations and powder diffraction detected several phase transitions:

$$G_3 \xrightarrow{550\ \text{K}} G_2 \xrightarrow{606\ \text{K}} G_1 \xrightarrow{843\ \text{K}} G_0$$

The $G_3 \rightarrow G_2$ transition is a first-order transition. The G_3 and G_2 phases are polar, optically uniaxial, moreover, the G_2 phase also shows optical activity.

Crystals of the composition $RbLiCrO_4$ are related to the $MLiAX_4$ family where M = K, Rb, Cs, NH_4 and AX_4 = BeF_4, SO_4, CrO_4. The atomic structure of the crystals can be described as being derived from β-tridymite. The structural characteristics and physical properties are best studied for the case of $KLiSO_4$ crystals. A list of publications on $KLiSO_4$ crystals can be found elsewhere (Schulz, Zucker & Frech, 1985; Klapper, Hahn & Chung, 1987).

The present study was undertaken in order to determine and refine the crystal structure of the G_3 and G_2 phases of $RbLiCrO_4$ and to establish the character of the twinning and the thermal vibration of atoms at various temperatures.

Experimental

G_3 phase

Single crystals of $RbLiCrO_4$ were grown from an aqueous solution of Rb_2CrO_4 and Li_2CrO_4. The diffraction experiment for the structure determination was performed on a CAD-4F Enraf–Nonius diffractometer with a graphite monochromator using Mo $K\alpha$ radiation and $\theta/2\theta$ scanning. The measurements were carried out on three spherical single-crystal specimens 0.0280 (5) cm in diameter [specimen (I) at 293 K], 0.0260 (5) cm [specimen (II) at 428 and 493 K] and 0.0220 (5) cm [specimen (III) at 523, 553 and 583 K]. The main crystallographic characteristics are listed in Table 1.* Lattice parameters were determined by least-squares refinement using 25 reflections with $21 < \theta < 33°$ in the G_3 phase and with $10 < \theta < 21°$ in the G_2 phase. The intensity measurements were made within the complete reflection sphere in reciprocal space at 428 K only, the measurements at all other temperatures were performed within a reflection hemisphere ($h \geq 0$, $\pm k$, $\pm l$).

The main difficulty concerning the symmetry and structure determination for the $RbLiCrO_4$ crystals was associated with twinning by merohedry. Such twinning is characterized by the exact coincidence of the reciprocal lattices of twin domains (Donnay & Donnay, 1974). Conventional analysis of the diffraction pattern geometry and the reflection intensities obtained from a specimen with equal (or almost equal) total volumes of domain variants inevitably leads to overestimation of the crystal symmetry. For

* Lists of structure factors and anisotropic thermal parameters have been deposited with the British Library Document Supply Centre as Supplementary Publication No. SUP 55446 (73 pp.). Copies may be obtained through The Technical Editor, International Union of Crystallography, 5 Abbey Square, Chester CH1 2HU, England. [CIF reference: SH0006]

0108-7681/93/010019-10$06.00

Table 1. *Crystallographic data obtained for three* $RbLiCrO_4$ *specimens* [(I)–(III)] *at different temperatures*

Reliability factors: $wR^2 = \sum_{hkl} w(F_{obs} - F_{calc})^2 / \sum_{hkl} wF_{obs}^2$; $R = \sum_{hkl} |F_{obs} - F_{calc}| / \sum_{hkl} F_{obs}$, where weights $w = 1/\sigma^2(F_{obs})$ and σ are the standard deviations of intensities obtained from counting statistics.

	293 K (I)	428 K (II)	493 K (II)	523 K (III)	553 K (III)	583 K (III)
Space group	$P31c$	$P31c$	$P31c$	$P31c$	$P6_3$	$P6_3$
Z	2	2	2	2	2	2
a (Å)	5.4021 (9)	5.423 (1)	5.438 (1)	5.453 (1)	5.463 (1)	5.471 (1)
c (Å)	9.175 (1)	9.161 (1)	9.160 (2)	9.151 (1)	9.147 (2)	9.140 (4)
V (Å^3)	231.89	233.32	234.64	235.68	236.39	236.95
D_x (g cm^{-3})	2.984	2.966	2.949	2.936	2.927	2.920
Max. $\sin\theta/\lambda$ (Å^{-1})	1.00	1.00	1.00	0.77	0.72	0.74
Reciprocal space	$+h, \pm k, \pm l$	$\pm h, \pm k, \pm l$	$+h, \pm k, \pm l$	$+h, \pm k, \pm l$	$+h, \pm k, \pm l$	$+h, \pm k, \pm l$
Reflections measured	2870	4680	1988	1641	1560	1511
Unique reflections ($I \geq 3\sigma_I$)	911	823	632	440	379	379
R_{av}	0.030	0.044	0.062	0.055	0.080	0.136
μ (cm^{-1})	134.7	133.9	133.2	132.6	132.2	131.9
V_1/V_2	3.4:1	8.3:1	8.3:1	1.2:1	1.6:1	1.6:1
g*	0.551×10^{-4}	0.417×10^{-4}	0.397×10^{-4}	0.408×10^{-4}	0.378×10^{-4}	0.382×10^{-4}
wR	0.029	0.021	0.027	0.035	0.034	0.046
R	0.033	0.026	0.034	0.037	0.035	0.043

* Isotropic extinction correction, Becker & Coppens formalism, type I, Lorentzian distribution.

a specimen with two domain variants, the total intensity of the hkl reflection is

$$F(hkl)^2 = (V_1 + V_2)^{-1}[V_1F_1(hkl)^2 + V_2F_2(h'k'l')^2],$$

where V_1 and V_2 are the volumes of the first and second domain variants and F_1^2 and F_2^2 are the contributions of these domain variants to the superimposing reflections. If $V_1:V_2 = 1:1$, $F(hkl)^2 = F(h'k'l')^2$ and the diffraction symmetry is overestimated. Twinning by merohedry can be of two types (Catti & Ferraris, 1976): type I or inversion twinning when the twin element is included in the Laue symmetry of the twin domain and the Laue classes of the twinned crystal and the twin domain coincide, and type II, when the twin element is not contained in the Laue symmetry of the twin domain but is a symmetry element of the crystal lattice.

Analysis of the diffraction pattern obtained from the G_3 phase shows the systematic absence of $hh\bar{2}hl$ reflections with $l \neq 2n$ which corresponds to the diffraction symbol $P{-}{-}c$, two Laue classes – $\bar{3}1m$ and $6/mmm$, and five space groups – $P31c$, $P\bar{3}1c$, $P\bar{6}2c$, $P6_3mc$ and $P6_3/mmc$. The absence of a centre of inversion (the G_3 phase shows the signal of the second optical harmonic) reduces the number of possible space groups to three – $P31c$, $P\bar{6}2c$ and $P6_3mc$. Finally, upon refinement of the structure models and with due regard to anomalous scattering and the twinning by merohedry, space group $P31c$ was chosen.

The point group $3m$, used to describe the $RbLiCrO_4$ crystals, is a subgroup of index 4 of the lattice point group $6/mmm$ (holohedry). In this case, four variants of twin domains and three laws of twinning by merohedry, $2 \parallel [001]$, $m \perp [001]$ and $\bar{1}$, are possible. If the specimen under study contains twin domains of two orientations related by the symmetry axis $2 \parallel [001]$ and if the total volumes of such domains are equal, the crystal symmetry is somewhat overestimated, *i.e.* $6mm$. If domains are related by the symmetry plane $m \perp [001]$, the crystal symmetry is also overestimated, *i.e.* $\bar{6}2m$. In both cases the Laue class is the same, $6/mmm$, but even for equal volumes of domain variants one can distinguish between the two cases above by allowing for anomalous scattering. If twin domains are related by the centre of inversion $\bar{1}$ (for the point group $3m$ this is equivalent to the action of the symmetry axis $2 \perp [001]$), then the twinned crystals also acquire higher symmetry, $\bar{3}m$, and the Friedel pairs of reflections have equal intensities even in the presence of substantial anomalous scattering. The simultaneous presence of the equal-volume domain variants with four different orientations results in overestimation of the crystal symmetry to the more symmetric group, $6/mmm$.

Table 2 lists the agreement factors R_{av} resulting from averaging of the diffraction intensities for the three specimens in the G_3 phase,

$$R_{av} = \sum_k [\sum_j (I_m - I_j)^2]_k / \sum_k \sum_j (I_j^2)_k,$$

where I_m is the averaged intensity, I_j is the intensity of measurement j, $\sum_j$ is the sum over symmetric equivalent group of reflections, and $\sum_k$ is the sum over symmetric independent reflections. Intensity averaging was performed within the $31m$, $6mm$, $\bar{6}2m$, $\bar{3}1m$ and $6/mmm$ groups. In averaging within the $31m$, $6mm$ and $\bar{6}2m$ groups the pairs of Friedel reflections were not averaged. Averaging within the centrosymmetric $\bar{3}1m$ and $6/mmm$ groups also included averaging of Friedel pairs. Comparing the R_{av} factors for different types of averaging favours the point group $31m$ (and the space group $P31c$) for the G_3 phase of the $RbLiCrO_4$ crystals. Analysis of the results illustrates the strong effect anomalous scattering has on the diffraction intensities. Inclusion

Table 2. *R_{av} values for the G_3 phase calculated within 31m, 6mm, $\bar{6}2m$ groups (Friedel pairs not averaged) and $\bar{3}1m$, 6/mmm groups*

Numbers N_i of averaged reflections with $I \geq 3\sigma_I$, and wR values in the refinement (with no allowance for anharmonicity) for the models: (*a*) with the space group $P31c$ without allowance for twinning, (*b*) with the twin element 2 ∥ [001], (*c*) with the twin element $m \perp$ [001], (*d*) with the twin element $\bar{1}$.

Point group	293 K (I)		428 K (II)		493 K (II)		523 K (III)	
	R_{av}/N_i	wR	R_{av}/N_i	wR	R_{av}/N_i	wR	R_{av}/N_i	wR
31*m*	0.030/911	0.042[a]	0.044/823	0.025[a]	0.062/632	0.031[a]	0.055/440	0.054[a]
6*mm*	0.069/629	0.034[b]	0.096/551	0.023[b]	0.101/427	0.030[b]	0.062/313	0.036[b]
$\bar{6}2m$	0.067/551	0.029[c]	0.096/475	0.022[c]	0.108/375	0.029[c]	0.076/268	0.046[c]
$\bar{3}1m$	0.061/532	0.039[d]	0.062/461	0.025[d]	0.073/364	0.031[d]	0.080/259	0.054[d]
6/*mmm*	0.076/339	–	0.100/312	–	0.109/250	–	0.080/180	–

of Friedel pairs in the averaging procedure (the data for the group $\bar{3}1m$ in Table 2) results in a substantial increase of the R_{av} values for all three specimens. This indicates that in all three specimens the centre of inversion cannot be a twin element. Comparison of the R_{av} values for the $\bar{6}2m$ and 6*mm* groups shows that for specimen (I) this factor is minimal in the $\bar{6}2m$ group. Thus the most probable twin element is the plane $m \perp$ [001]. For specimen (II), averaging did not reveal any preferred symmetry group. For specimen (III), the minimum R_{av} value obtained was for the group 6*mm* and the most probable twin element seems to be the axis 2 ∥ [001].

Final refinement of the structure model for the G_3 phase was performed within the $P31c$ group with allowance for twinning by merohedry. The number N_i of symmetrically nonequivalent reflections for this group (the Friedel pairs were not averaged) was 911, 823, 632 and 440 at 293, 428, 493 and 523 K, respectively.

G_2 phase

The diffraction pattern from the G_2 phase only showed the systematic absences: 000*l* reflections with $l \neq 2n$ which corresponds to the diffraction symbol $P6_3$––, two Laue classes – 6/*m* and 6/*mmm*, and three space groups – $P6_3$, $P6_3/m$ and $P6_322$. If one takes into account that the G_2 phase is noncentrosymmetric (observed from the second optical harmonic and optical activity), then the space group is chosen uniquely as $P6_3$. When refining the structure model of the crystals, one should necessarily take into account possible twinning by merohedry of the specimens. The point group 6 of the G_2 phase is a subgroup of index 4 of the 6/*mmm* group of the lattice. This leads to four possible orientations of twin domains and three laws of twinning by merohedry. The twin elements in the G_2 phase can be the plane m ∥ [001] [plane (10$\bar{1}$0) or (11$\bar{2}$0)], the axis 2 $\perp$ [001] (2 ∥ [100] or [110]) or the centre of inversion $\bar{1}$, which is equivalent to the plane $m \perp$ [001] in the case of group 6 of the crystals. Therefore, if the volumes of two domain variants are equal, the symmetry of the twinned crystal will be overestimated – 6*mm*, 622 or 6/*m*. If the specimen under study has four types of twin domains, the symmetry is raised to 6/*mmm*. The Laue class for groups 6*mm* and 622 is 6/*mmm*, but these two cases can be distinguished from each other in the presence of anomalous scattering. Twinning in the $KLiSO_4$ phase with symmetry $P6_3$ was considered by Klapper, Hahn & Chung (1987) from the results of optical, pyroelectric and X-ray topographic data.

Table 3. *R_{av} values for the G_2 phase calculated within the 6, 6mm, 622 groups (Friedel pairs not averaged) and 6/m, 6/mmm groups*

Numbers N_i of averaged reflections with $I \geq 3\sigma_I$, and wR values calculated in the refinement (with no allowance for anharmonicity) for the models: (*a*) with the space group $P6_3$ without allowance for twinning, (*b*) with the twin element m ∥ [001], (*c*) with the twin element 2 $\perp$ [001], (*d*) with the twin element $\bar{1}$.

Point group	553 K (III)		583 K (III)	
	R_{av}/N_i	wR	R_{av}/N_i	wR
6	0.080/379	0.050[a]	0.136/379	0.063[a]
6*mm*	0.083/308	0.039[b]	0.137/301	0.049[b]
622	0.097/240	0.043[c]	0.169/234	0.052[c]
6/*m*	0.096/246	0.050[d]	0.168/244	0.063[d]
6/*mmm*	0.097/180	–	0.169/177	–

Table 3 lists the R_{av} factors obtained from averaging the diffraction intensities of specimen (III) at 553 and 583 K. The intensities were averaged within the groups 6, 6*mm*, 622, 6/*m* and 6/*mmm*. Averaging within groups 6, 6*mm* and 622 did not take the Friedel pairs of reflections into account. Averaging within the 6/*m* and 6/*mmm* groups also included the Friedel pairs. Analysis of the R_{av} factors showed a substantial effect of anomalous scattering on the diffraction intensities, thus excluding the centre of inversion as a possible twin element. Comparing the R_{av} values obtained from intensity averaging within groups 6*mm* and 622, we see that the minimum R_{av} value is attained within the 6*mm* group, thus dictating the choice of the symmetry plane m ∥ [001] as a twin element.

Final refinement of the structural model for the G_2 phase was performed within the $P6_3$ group. The number N_i of symmetrically nonequivalent reflec-

tions in this group (the Friedel pairs of reflections were not averaged) is 379 at 553 and 583 K.

Experimental diffraction intensities obtained at all the temperatures were corrected for Lp factor and absorption. All structural computations, including structure refinements by the least-squares technique with allowance for the experimental weighting factors, were carried out using the *PROMETHEUS* system of programs (Zucker, Perenthaler, Kuhs, Bachmann & Schulz, 1983) and with the atomic scattering curves and dispersion corrections $\Delta f'$ and $\Delta f''$ (for Rb, Cr and O atoms) from *International Tables for X-ray Crystallography* (1974, Vol. IV). Extinction was taken into account in the isotropic approximation according to the formalism of Becker & Coppens (1974) (type I, Lorentzian distribution).

Structure refinements

G_3 phase

The initial model used for refinement of the G_3 phase of the $RbLiCrO_4$ crystals at 293 K was based on the atomic coordinates of the $KLiSO_4$ structure at 298 K (Karppinen, Lundgren & Liminga, 1983); at other temperatures it was based on the parameters obtained for $RbLiCrO_4$ at lower temperatures. At 298 K $KLiSO_4$ crystals are characterized by the space group $P6_3$. The structural models considered in the space groups $P31c$ and $P6_3$ differ by the mutual orientations of layers built up of six-membered rings of alternating $[CrO_4]$ and $[LiO_4]$ tetrahedra (Fig. 1). Both models consist of alternating pairs of such layers. The structures of the layers themselves are identical but the effect of the symmetry elements on the layer is different: in group $P6_3$ the first layer is transformed into the second by the 2_1 axis, whereas in $P31c$ it is transformed by the glide plane c. The $[CrO_4]$ tetrahedra of the first layer share vertices [the O(1) atoms] with the $[LiO_4]$ tetrahedra of the second layer. The $[CrO_4]$ and $[LiO_4]$ tetrahedra have opposite orientations with respect to the main symmetry axis of the structure. The unit cell of the crystal contains two $[CrO_4]$ and two $[LiO_4]$ tetrahedra. The Rb atoms lie on the main symmetry axes in channels formed by the six-membered rings.

Refinement of the atomic coordinates and thermal vibration parameters in the anisotropic approximation in the space group $P31c$ yielded the following reliability factors: $wR = 0.042$, 0.025, 0.031 and 0.054 at 293, 428, 493 and 523 K, respectively. Analysis of the difference electron density maps constructed at this stage proved the presence of residual density peaks in the plane of the O(2) atoms forming the base of the tetrahedral groups (Fig. 2). Three such peaks of residual density form a triangle around the threefold axis with an area equal to that of the triangle made up of the O(2) atoms but rotated by about 60°. The values of these peaks differ substantially for the different specimens under study. The residual density can be interpreted as being due to the presence of domains of different orientations. An

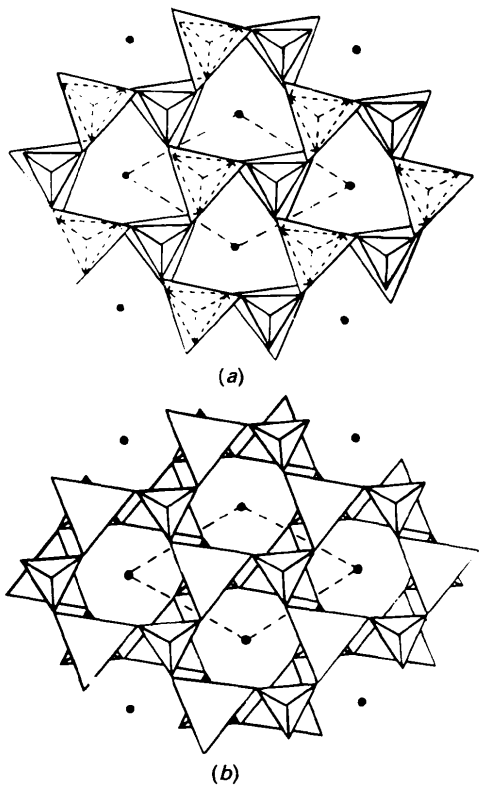

Fig. 1. Projection along the [001] direction of (*a*) the G_3 and (*b*) the G_2 phases of $RbLiCrO_4$ crystals. Small tetrahedra represent $[CrO_4]$ groups, large tetrahedra represent $[LiO_4]$ groups, full circles indicate Rb atoms. The unit cell is shown by dashed lines.

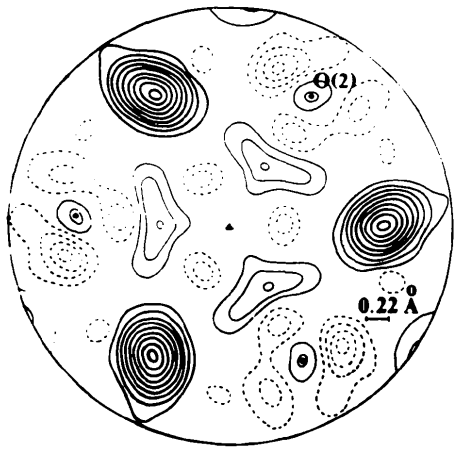

Fig. 2. The *xy* section of the residual electron density passing through the O(2) atoms at 293 K. Untwinned model. Contours of equal densities are drawn at intervals of 0.33 e $Å^{-3}$.

analogous domain structure was also observed in $KLiSO_4$ crystals by Karppinen, Lundgren & Liminga (1983).

It should be emphasized that for any of the domain variants considered above the location of the residual electron density peaks relative to those of the O(2) atoms is very close to that shown in Fig. 2. Twinning that occurs due to symmetry axes or planes results in a different combination of domain variants and produces a particular effect on the anomalous-scattering contribution to the reflection intensities. If the influence of the anomalous scattering is small, the absolute configurations of the components cannot be distinguished and the twinning nature cannot be determined unambiguously. When constructing difference electron density maps without allowing for twinning, the calculated structure factors and their phases are determined from the configuration of the domain variant having the larger volume. Then the specific features of the difference electron density distribution show only the presence of the neglected twinning effect.

In the G_3 phase any of the following domain variants are possible: xyz, $xy\bar{z}$, $\bar{x}yz$ and $\bar{x}\bar{y}\bar{z}$, corresponding to twinning by a plane, the symmetry axis 2, and the centre of inversion. For all the specimens, the structure models were refined with due regard for possible twinning by all these laws. In order to take possible twinning in the specimen into account, it is necessary to determine the volume ratio of the domain variants and to separate the contribution of the component with the larger volume in the experimental intensities. In other words, it is necessary to add a parameter $p = V_1/V_2$ into the refinement procedure. The problems indicated above were solved by the method suggested by Sirota & Maksimov (1984).

Table 2 lists the wR factors obtained from the structure refinements obtained with due regard for the different possible twin laws. The minimum wR values for specimen (I) at 293 K and specimen (II) at 428 and 493 K (0.029, 0.022, 0.029, respectively) were obtained for the twin law $m \perp [001]$, *i.e.* hkl and $hk\bar{l}$ reflections from different twin domains superimposed. It should be noted that the wR factor calculated with allowance made for twinning reduces more pronouncedly for specimen (I) than for specimen (II), which is explained by the different volume ratios, which are for specimens (I) and (II) $V_1:V_2 =$ 3.4:1 and 8.3:1, respectively.

The minimum value of $wR = 0.036$ for specimen (III) at 523 K was obtained for the twin law $2 \parallel [001]$ with the volume ratio of twin components being $V_1:V_2 = 1.2:1$.

Inversion twinning with superposition of the hkl and $\bar{h}\bar{k}\bar{l}$ reflections is almost impossible. Analysis of the diffraction patterns showed substantially different intensities for Friedel pairs of reflections. Refinement of the structural models with due regard for inversion twinning (performed so as to verify the models) did not reduce the wR factors.

Finally, we also checked for the possibility of the simultaneous existence of domains with three orientations in the specimens. However, refinement of the relevant models yielded zero volume for the third domain variant. It is therefore possible to state that, within the accuracy of our experiment and calculations, all three specimens have twin domains with only two orientations. If the twin component with the larger volume in specimen (I) is denoted by xyz, then the second component can be written as $xy\bar{z}$; specimen (II) has the components $\bar{x}\bar{y}\bar{z}$ and $\bar{x}yz$, and specimen (III) includes components $xy\bar{z}$ and $\bar{x}\bar{y}\bar{z}$, respectively.

Taking the above twin laws into account, it is possible to construct models of the twin boundaries in the $P31c$ phase. Such constructions are based on the assumption that the tetrahedral framework of the structure is also continuous at the twin boundaries and that the direct linking of two $[CrO_4]$ or two $[LiO_4]$ tetrahedra is forbidden. Similar hypotheses were also put forward by Klapper, Hahn & Chung (1987) in the construction of twin boundary models for $KLiSO_4$ crystals described by the group $P6_3$. Consider twinning where domains are related by the symmetry plane $m \perp [001]$. Within the framework of the assumption mentioned above, the only possible variant here is the boundary parallel to the $(10\bar{1}0)$ plane (Fig. 3). This model does not require large atomic displacements in the vicinity of the boundary, the most noticeable changes involve the environment of the Rb atoms. Inside the twin domains, the Rb atom is surrounded by nine O atoms. Coordination numbers for the Rb atoms in the plane of the twin boundary are either 8 or 10. If domains are related by the symmetry operation $2 \parallel [001]$, the twin boundary can be parallel to the (0001) (Fig. 4*a*) or $(10\bar{1}0)$ (Fig. 4*b*) planes. But the boundary parallel to the (0001) plane is more favourable since its formation

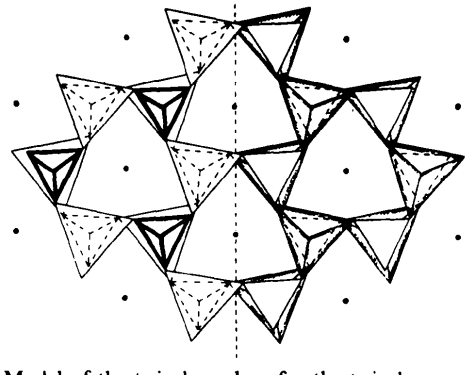

Fig. 3. Model of the twin boundary for the twin law $m \perp [001]$. The boundary parallel to $(10\bar{1}0)$ is shown by a dashed line.

does not require substantial displacement of atoms in the vicinity of the twin boundary and the coordination number 9 of the Rb atoms is preserved. The junction of the twin domains parallel to the $(10\bar{1}0)$ plane requires substantial displacement of the atoms in the vicinity of the twin boundary and at the boundary itself it is equal to **q** (Fig. 4), whereas the coordination number of the Rb atoms increases up to 11 oxygens. If domains are related through the centre of inversion, the most probable variant is the boundary parallel to the $(10\bar{1}0)$ plane (Fig. 5). But in this case as well, formation of the boundary requires atomic displacements in its vicinity and an increase in the coordination number of the Rb atoms in the boundary plane to 10 or 12.

Comparing the models of twin boundaries in the $P31c$ phase with those in the $P6_3$ phase of $KLiSO_4$ (Klapper, Hahn & Chung, 1987), one can readily see that the structure of the boundary parallel to the (0001) plane in the $P31c$ phase (twin element 2 ‖ [001]) (Fig. 4*a*) coincides with the structure of the $P6_3$ phase (Fig. 1*b*) and *vice versa* [Fig. 11*a* of Klapper, Hahn & Chung (1987)].

When studying the $KLiSO_4$ crystals, special attention was paid to disordering of the O(1) and O(2) atoms (Karppinen, Lundgren & Liminga, 1983; Bhakay-Tamhane, Sequeira & Chidambaram, 1984; Schulz, Zucker & Frech, 1985). The point is that, in the first approximation, both the static disorder of atoms and the real anharmonicity of atomic thermal vibrations in the process of structure refinement manifest themselves in the same way. We refined the thermal vibration parameters in the anharmonic approximation for all atoms [Rb, Cr, O(1), O(2)] except for Li, using the formalism of the Gram–Charlier expansion of the probability density function (PDF) (Muradyan, Sirota, Makarova & Simonov, 1985). In this case, the temperature factor, with allowance made for anharmonicity, can be written in terms of the Fourier transform of the probability density distribution with retention of not only the harmonic terms but also the anharmonic terms of third and higher orders. In the refinements we took account of the temperature factor expansion tensors up to fourth order.

As a result of refinement of the thermal parameters for the Rb atom in the anharmonic approximation we have revealed the only significant parameter C^{111} of the Rb atom. Fig. 6 shows a section of the residual electron density constructed from the refined thermal parameters of the Rb atom in the harmonic approximation. At all four tempera-

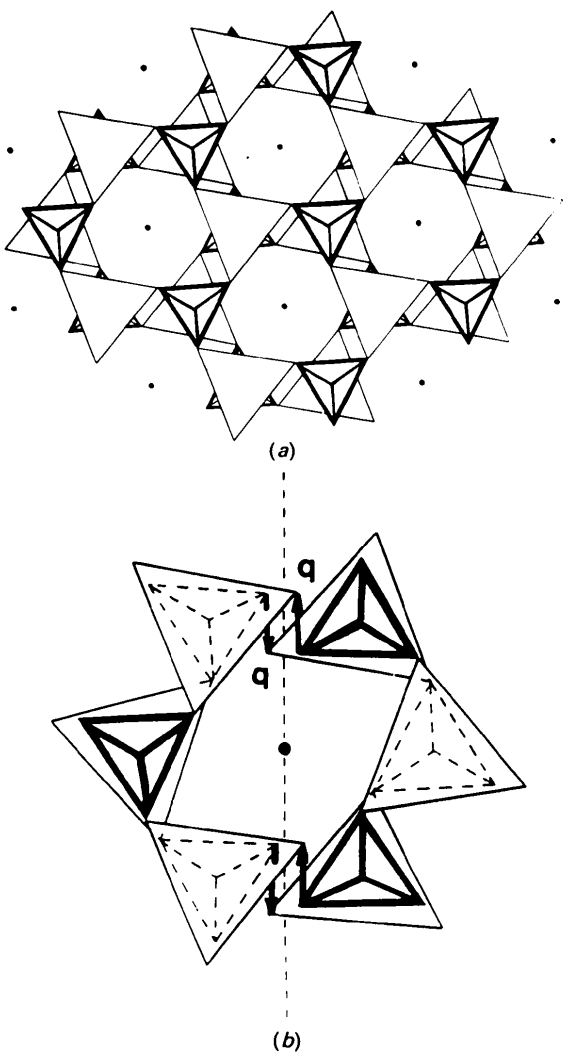

Fig. 4. Models of twin boundaries for the twin law 2 ‖ [001]. (*a*) Boundary parallel to (0001). The twin boundary lies between two tetrahedral layers. (*b*) Boundary parallel to $(10\bar{1}0)$.

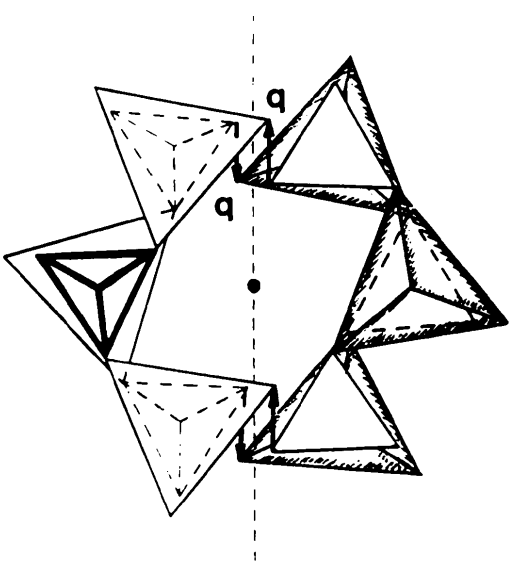

Fig. 5. Model of the twin boundary for the twin law $\bar{1}$. Boundary is parallel to $(10\bar{1}0)$.

Table 4. *Refined structural parameters for* $RbLiCrO_4$

Positional parameters are given in fractional coordinates. Thermal parameters B^{ij} (Å^2) are defined by the temperature-factor equation $T(H) = \exp[-(h^2B^{11} + k^2B^{22} + l^2B^{33} + 2hkB^{12} + 2hlB^{13} + 2klB^{23})]$. For the Rb, Li, Cr and O(1) atoms $B^{11} = B^{22}$, $B^{12} = B^{11}/2$, $B^{13} = B^{23} = 0$. C^{ijk} ($\times 10^3$) are anharmonic parameters. Estimated standard deviations are given, in parentheses, on the last quoted place.

		293 K	428 K	493 K	523 K	553 K	583 K
Rb	B^{11}	0.02224 (8)	0.0327 (1)	0.0398 (2)	0.0451 (4)	0.0468 (5)	0.0509 (6)
	B^{33}	0.00491 (3)	0.00704 (5)	0.00871 (8)	0.0103 (2)	0.0111 (2)	0.0122 (2)
	C^{111}	0.0045 (7)	0.0094 (9)	0.013 (2)	0.020 (4)	0.020 (4)	0.024 (4)
	C^{112}	0	0	0	0	0	0.012 (6)
Li	z	0.682 (1)	0.684 (1)	0.683 (2)	0.680 (3)	0.680 (4)	0.682 (5)
	B^{11}	0.029 (2)	0.049 (3)	0.052 (5)	0.042 (7)	0.044 (8)	0.045 (9)
	B^{33}	0.008 (1)	0.008 (1)	0.011 (3)	0.014 (5)	0.016 (5)	0.015 (6)
Cr	z	0.2951 (1)	0.2940 (1)	0.2931 (2)	0.2925 (3)	0.2920 (3)	0.2917 (4)
	B^{11}	0.01166 (9)	0.0171 (1)	0.0215 (2)	0.0239 (4)	0.0255 (5)	0.0274 (7)
	B^{33}	0.00293 (4)	0.00424 (6)	0.0053 (1)	0.0063 (2)	0.0066 (2)	0.0074 (3)
O(1)	z	0.4731 (4)	0.4721 (5)	0.4706 (8)	0.4678 (9)	0.469 (2)	0.470 (2)
	B^{11}	0.043 (1)	0.068 (2)	0.080 (3)	0.082 (5)	0.085 (5)	0.097 (7)
	B^{33}	0.0030 (3)	0.0040 (4)	0.0050 (7)	0.008 (2)	0.008 (2)	0.009 (2)
O(2)	x	0.3864 (5)	0.3922 (5)	0.3951 (7)	0.3973 (9)	0.409 (1)	0.401 (2)
	y	0.3490 (5)	0.3537 (4)	0.3567 (7)	0.3613 (9)	0.368 (1)	0.365 (1)
	z	0.2387 (4)	0.2372 (3)	0.2357 (5)	0.2337 (7)	0.2345 (8)	0.2349 (9)
	B^{11}	0.0193 (8)	0.0262 (9)	0.032 (2)	0.036 (3)	0.055 (3)	0.053 (4)
	B^{22}	0.0192 (8)	0.0309 (9)	0.039 (2)	0.042 (3)	0.038 (3)	0.038 (3)
	B^{33}	0.0096 (3)	0.0129 (3)	0.0166 (6)	0.023 (1)	0.024 (1)	0.024 (1)
	B^{12}	0.0059 (3)	0.0093 (8)	0.012 (1)	0.011 (2)	0.007 (2)	0.009 (3)
	B^{13}	0.0041 (3)	0.0052 (4)	0.0063 (8)	0.005 (1)	0.005 (2)	0.005 (2)
	B^{23}	0.0032 (4)	0.0046 (5)	0.0061 (8)	0.009 (2)	0.010 (2)	0.010 (2)
	C^{111}	0	0	0	0	0.010 (2)	0.000 (2)
	C^{113}	0	0	0	0	0.04 (1)	0.04 (2)
	C^{133}	0	0	0	0	0.033 (6)	0.034 (7)
	C^{123}	0	0	0	0	0.027 (9)	0.024 (9)

tures, the residual electron density maps in the vicinity of the Rb atom show three positive and three negative extrema. Adding the C^{111} parameter of the Rb atom to the refined parameters, we managed to reduce the wR factors from 0.0292 to 0.0287 at 293 K, from 0.0224 to 0.0212 at 428 K, from 0.0291 to 0.0269 at 493 K and from 0.0361 to 0.0350 at 523 K. Such reductions in the wR values ensure a significant level of improvement in fit, $\alpha < 0.005$ according to the test of Hamilton (1965). Fig. 7 depicts a section of the difference PDF of the Rb atom, which shows the contribution of the anharmonic parameters. It was calculated from the refined C^{111} parameter of the Rb atom. Three negative peaks on the difference PDF in the vicinity of the Rb atom are displaced towards the three closest O(1) atoms. The sections of the electron density distribution and difference PDF are given at $T = 428$ K. At all other temperatures, the distributions are similar to those depicted in Figs. 6 and 7.

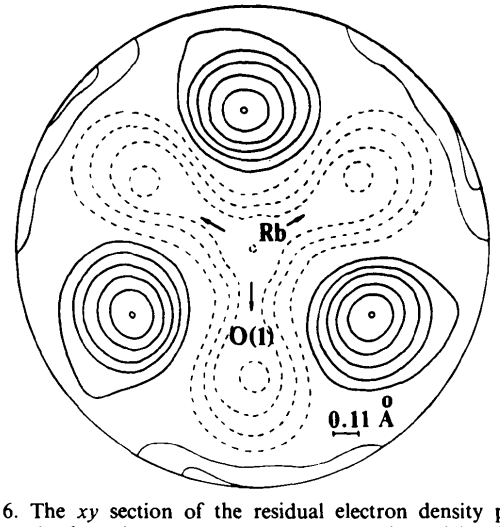

Fig. 6. The xy section of the residual electron density passing through the Rb atom at 428 K. Twinned model. Thermal vibrations of the Rb atom are for the harmonic approximation. Contours of equal densities are drawn at intervals of 0.2 e Å^{-3}.

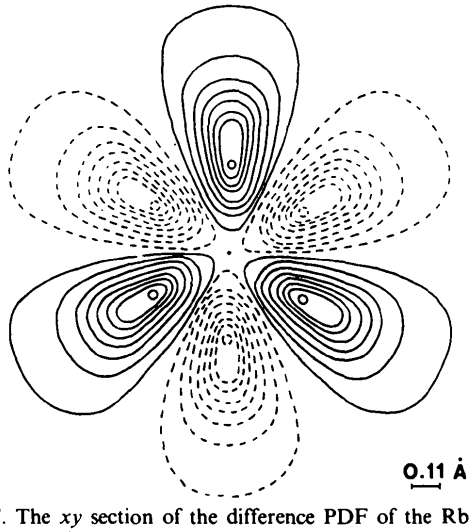

Fig. 7. The xy section of the difference PDF of the Rb atom at 428 K, which shows the deviations from a purely harmonic PDF and is calculated from the refined third-order anharmonic terms.

Table 5. *Main interatomic distances* (Å) *and valence angles* (°) *in* $RbCrLiO_4$

		293 K	428 K	493 K	523 K	553 K	583 K
Cr—O(1)		1.633 (4)	1.631 (4)	1.626 (6)	1.60 (1)	1.62 (1)	1.63 (2)
Cr—O(2)	× 3	1.642 (2)	1.632 (2)	1.632 (3)	1.641 (5)	1.599 (5)	1.629 (7)
Cr—Li	× 3	3.286 (4)	3.290 (4)	3.299 (6)	3.312 (9)	3.32 (1)	3.31 (1)
Li—O(1)		1.92 (1)	1.94 (1)	1.94 (2)	1.94 (3)	1.93 (3)	1.94 (4)
Li—O(2)	× 3	1.946 (4)	1.940 (4)	1.938 (6)	1.93 (1)	1.94 (1)	1.93 (1)
Rb—O(1)	× 3	3.1287 (4)	3.1414 (4)	3.1512 (6)	3.162 (1)	3.167 (1)	3.170 (1)
Rb—O(2)	× 3	2.962 (3)	2.974 (2)	2.978 (4)	2.980 (5)	3.024 (6)	3.005 (7)
Rb—O(2′)	× 3	3.118 (3)	3.150 (3)	3.174 (4)	3.200 (6)	3.231 (7)	3.208 (9)
O(1)—Cr—O(2)		108.4 (1)	108.6 (1)	108.8 (2)	109.1 (3)	109.2 (3)	108.6 (4)
O(2)—Cr—O(2′)		110.6 (1)	110.3 (1)	110.1 (2)	109.8 (2)	109.7 (3)	110.3 (4)
O(1)—Li—O(2)		105.4 (4)	104.6 (4)	104.5 (6)	104.7 (9)	104.7 (1.0)	104.4 (1.3)
O(2)—Li—O(2′)		113.2 (3)	113.9 (3)	113.9 (5)	113.8 (8)	113.8 (8)	114.1 (1.1)

Table 6. *Thermal vibration ellipsoids*

B_{eq} (Å^2) are equivalent isotropic thermal parameters calculated from the volumes of the thermal vibration ellipsoids. u_i (Å) – semi-major axes.

		293 K	428 K	493 K	523 K	553 K	583 K
Rb	B_{eq}	1.850 (8)	2.712 (8)	3.33 (1)	3.83 (2)	4.03 (2)	4.41 (3)
	u_1	0.1447 (6)	0.1730 (6)	0.1924 (9)	0.209 (2)	0.217 (2)	0.227 (2)
	$u_2 = u_3$	0.1570 (4)	0.1912 (3)	0.2115 (6)	0.2257 (7)	0.2303 (7)	0.241 (1)
Li	B_{eq}	2.6 (2)	3.8 (2)	4.3 (3)	4.1 (5)	4.4 (5)	4.4 (6)
	u_1	0.19 (2)	0.18 (2)	0.22 (2)	0.25 (4)	0.26 (4)	0.25 (5)
	$u_2 = u_3$	0.180 (8)	0.234 (6)	0.242 (9)	0.22 (1)	0.22 (2)	0.23 (2)
Cr	B_{eq}	1.010 (8)	1.481 (8)	1.87 (1)	2.12 (2)	2.26 (2)	2.46 (3)
	u_1	0.112 (1)	0.134 (1)	0.151 (2)	0.164 (3)	0.167 (3)	0.177 (3)
	$u_2 = u_3$	0.1136 (5)	0.1382 (4)	0.1554 (7)	0.164 (1)	0.170 (1)	0.177 (2)
O(1)	B_{eq}	2.85 (6)	4.44 (7)	5.3 (1)	5.8 (2)	5.9 (2)	6.7 (3)
	u_1	0.113 (7)	0.130 (7)	0.15 (1)	0.19 (2)	0.18 (2)	0.19 (3)
	$u_2 = u_3$	0.219 (3)	0.275 (3)	0.300 (5)	0.305 (6)	0.311 (7)	0.331 (9)
O(2)	B_{eq}	2.34 (4)	3.32 (4)	4.14 (7)	5.2 (1)	6.2 (1)	6.0 (2)
	u_1	0.123 (4)	0.151 (3)	0.170 (5)	0.182 (8)	0.180 (8)	0.18 (1)
	u_2	0.171 (4)	0.209 (3)	0.228 (4)	0.248 (8)	0.299 (8)	0.29 (1)
	u_3	0.211 (3)	0.244 (3)	0.277 (5)	0.323 (8)	0.335 (8)	0.33 (1)

Our attempts to reveal deviations from harmonicity of the thermal vibrations of the O(1), O(2) and Cr atoms in the G_3 phase did not yield any significant anharmonic parameters.

The final positional and thermal parameters of the atoms in the $RbLiCrO_4$ structure (characterized by the space group $P31c$) obtained with due regard for twinning are listed in Table 4. The Rb atom occupies the 2(*a*) (000) position; the Li, Cr and O(1) atoms are in positions 2(*b*) ($\frac{2}{3}$, $\frac{1}{3}$, *z*); the O(2) atom occupies the general position (*xyz*). To facilitate comparison, the configurations of all the specimens in Table 4 are reduced to the *xyz* configuration of the component having the larger volume in specimen (I). The main interatomic distances and valence angles are shown in Table 5, parameters of the thermal vibration ellipsoids are listed in Table 6. The final structural model of $RbLiCrO_4$ has parameters close to those for the $P31c$ phase of $KLiSO_4$ at 200 K with an ordered arrangement of the O atoms (Zhang, Yan & Boucherle, 1988).

G_2 phase

Atomic coordinates for the initial model of the G_2 phase of $RbLiCrO_4$ were those determined by us for the G_3 phase at 523 K. As has been established, the G_2 phase is described by the space group $P6_3$. The difference between the $P31c$ and $P6_3$ structures reduces to the different mutual orientations of the layers constructed from six-membered rings. In fact, it is associated with rotation of the triangular base of a tetrahedron formed by O(2) atoms about the three-fold axis in one of the two layers (Fig. 1).

Refinement of the positional and thermal parameters in the anisotropic approximation within space group $P6_3$ yielded the *wR* factors 0.050 and 0.063 at 553 and 583 K, respectively. In a similar manner to the G_3 phase (Fig. 2), the residual electron density maps showed peaks forming a triangle in the plane of the O(2) atoms, which is typical of twinned crystals. For the G_2 phase, four orientations of twin domains are possible – *xyz*, $\bar{y}\bar{x}z$, $yx\bar{z}$ and $\bar{x}\bar{y}\bar{z}$ related by the twin elements $m \parallel [001]$, $2 \perp [001]$ and $\bar{1}$. Table 3 shows the *wR* factors obtained in the refinement taking account of the twinning by merohedry in specimen (III). The minimum *wR* values, $wR = 0.039$ and 0.049 at 553 and 583 K, respectively, were obtained for the variant with the domain orientations related by the symmetry plane $m \parallel [001]$ and superimposing *hkl* and $\bar{k}\bar{h}l$ reflections from twin domains. Refinement of the model obtained by adding a third domain orientation gave zero volume

for the component related to the larger component by the twin element 2 ⊥ [001].

If the larger component in specimen (I) is initially taken as having the configuration xyz, then specimen (III) at 523 K (G_3 phase) has the twin components $xy\bar{z}$ and $\bar{x}\bar{y}\bar{z}$, the volume ratio being $V_1:V_2 = 1.2:1$. Specimen (III) at 553 and 583 K, which is above the temperature required for phase transition to the G_2 phase, has the components $\bar{y}\bar{x}\bar{z}$ and $xy\bar{z}$, the volume ratio being $V_1:V_2 = 1.6:1$. Thus preservation of the optical axis orientation of the crystal in the $G_3 \rightarrow G_2$ phase transition is provided by preservation of the orientations of the $[CrO_4]$ and $[LiO_4]$ tetrahedra with respect to the 3 axis. The volume ratio of domain variants changed in this phase transition.

As for the G_3 phase, in the G_2 phase we also refined all thermal parameters except those of the Li atom with allowance made for anharmonicity. The residual electron density distribution in the vicinity of the Rb atom obtained upon refinement of the thermal parameters in the harmonic approximation is similar to that of the G_3 phase (Fig. 6). Refinement of the thermal parameters of the Rb atom in the anharmonic approximation showed that the only significant parameters are C^{111} at 553 K and C^{111} and C^{112} at 583 K. The difference PDF of the Rb atom in the G_2 phase is identical to that for the G_3 phase (Fig. 7). For the G_2 phase the following anharmonic parameters are also significant: C^{111}, C^{113}, C^{133} and C^{123} for the O(2) atom. In real space this results in maxima of the difference PDF of the O(2) atom in the plane normal to the threefold axis. This is in good agreement with the displacement of the O(2) atom observed in the phase transition. Adding two more parameters, C^{111} and C^{112} due to the Rb atom, the wR factors reduced from 0.0387 to 0.0376 at 553 K, and from 0.0486 to 0.0477 at 583 K. The addition of still another parameter, C^{ijk} due to the O(2) atom, reduced the wR values even more – to 0.0342 at 553 and 0.0464 at 583 K. The O(1) and Cr atoms showed no significant deviation of thermal vibration from harmonicity.

The final positional and thermal parameters of the atoms for the G_2 phase obtained with allowance made for twinning are given in Table 4. The configurations of the twin components are reduced to the xyz configuration of specimen (I). The main interatomic distances and valence angles are listed in Table 5, the parameters of the ellipsoids of thermal vibrations are given in Table 6. The crystallographic data obtained for $RbLiCrO_4$ evidence its isostructurality with $KLiSO_4$.

Discussion

Structural investigation of $RbLiCrO_4$ crystals has shown that the $G_3 \rightarrow G_2$ phase transition is accompanied by a change of space group from $P31c$ to $P6_3$. The most important atomic rearrangement in the phase transition reduces to a reconstruction of only one of the two layers forming the structure. The triangular bases of tetrahedra forming this layer are rotated by ~48° about the threefold axis. Allowance for the effect of anomalous scattering on the diffraction intensities provided the unambiguous determination of the twin laws for all the specimens under investigation, both in the G_3 and G_2 phases. Thus the twin element for specimen (III) below the phase transition is the symmetry axis 2 ‖ [001] and above is the symmetry plane m ‖ [001]. The

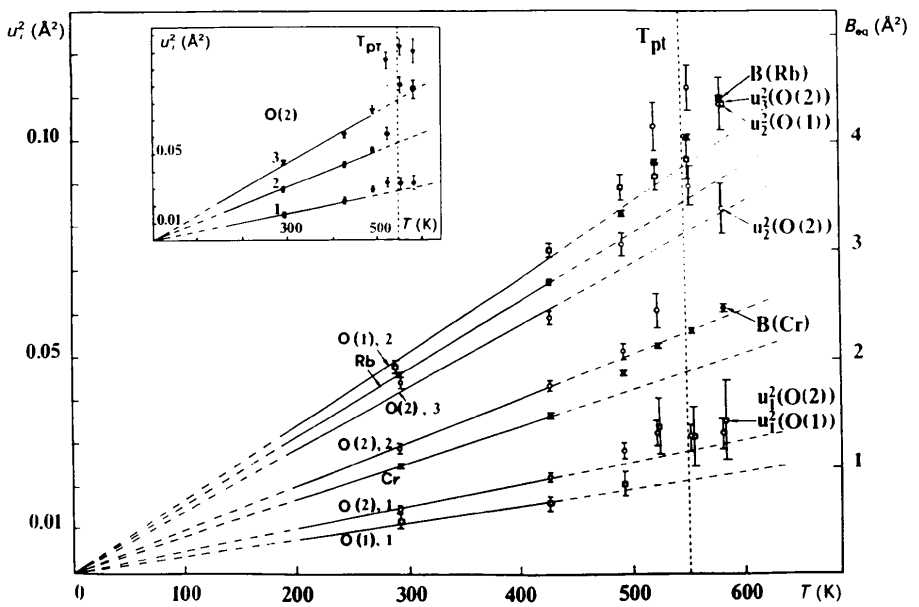

Fig. 8. The equivalent isotropic thermal parameters B_{eq} of the Rb and Cr atoms and mean-square displacements u_i^2 of the O(1) and O(2) atoms as functions of temperature.

direction of the main symmetry axis of the crystal is not changed in the phase transition, remaining parallel in the domains below and above the phase transition. The main difference between the twin components relates to in which layer the triangle formed by the O(2) atoms is rotated.

Analysis of the thermal vibration parameters of the atoms provided the obvious correlations between vibrational amplitudes and the strength and direction of the chemical bonds in the structure. Thus the semi-minor axes u_1 of the ellipsoids for the O(1) and O(2) atoms are aligned along the strongest Cr—O bonds. Both O atoms show strong anisotropy of thermal vibrations and the u_2 and u_3 parameters describing their thermal motion in the planes of the perpendicular Cr—O bonds have much larger values than u_1. Increasing temperature and the phase transition are accompanied by reduction of the anisotropy of thermal vibration for the Cr atom and simultaneous levelling of the thermal parameters of the O(1) and O(2) atoms along the Cr—O bonds.

Fig. 8 depicts the temperature dependence of the thermal parameters for $RbLiCrO_4$ (the equivalent isotropic thermal parameters B_{eq} for the Rb and Cr atoms with a small anisotropy of thermal vibration and parameters u_i^2 for the O atoms). Parameters of the Li atom are not shown because of their low accuracy. In comparison with the values at 293 K, the thermal parameters of all the atoms at 428 K increase almost proportionally to the changes in absolute temperature. As the phase transition is approached (T_{pt} = 550 K) the thermal parameters of $RbLiCrO_4$ increase drastically. This seems to be associated with the temperature dependence of the force constants in the vicinity of the phase-transition temperature. But the increase in the u_2^2 and u_3^2 parameters of the O(2) atom which rotates during the process of phase transition is clearly seen even against a background of such a drastic increase in thermal parameters. The anharmonic parameters of the O(2) atom obtained for the G_2 phase also indicate some 'softening' of the effective potential for this atom. Finer details in the behaviour of the thermal parameters of atoms in the structures of the type considered above can be established in separate neutron diffraction experiments.

The authors are grateful to Professor V. I. Simonov for many helpful discussions.

References

BECKER, P. J. & COPPENS, P. (1974). *Acta Cryst.* A**30**, 129–147.

BHAKAY-TAMHANE, S., SEQUEIRA, A. & CHIDAMBARAM, R. (1984). *Acta Cryst.* C**40**, 1648–1651.

CATTI, M. & FERRARIS, G. (1976). *Acta Cryst.* A**32**, 163–165.

DONNAY, G. & DONNAY, J. D. (1974). *Can. Mineral.* **12**, 422–425.

HAMILTON, W. C. (1965). *Acta Cryst.* **18**, 502–510.

KARPPINEN, M., LUNDGREN, J. O. & LIMINGA, R. (1983). *Acta Cryst.* C**39**, 34–38.

KLAPPER, H., HAHN, TH. & CHUNG, S. J. (1987). *Acta Cryst.* B**43**, 147–159.

KRUGLIK, A. I., MEL'NIKOVA, S. V., ALEKSANDROV, K. S. & GRANKINA, V. A. (1990). *Fiz. Tverd. Tela*, **32**, 3029.

KRUGLIK, A. I., MEL'NIKOVA, S. V., TOLOCHKO, B. P., MAKAROVA, I. P. & ALEKSANDROV, K. S. (1991). Preprint No. 680F of the L. V. Kirenskii Institute of Physics of the Siberian Division of the USSR Academy of Sciences, Krasnoyarsk, Russia.

MURADYAN, L. A., SIROTA, M. I., MAKAROVA, I. P. & SIMONOV, V. I. (1985). *Kristallografiya*, **30**, 258–266.

SCHULZ, H., ZUCKER, U. & FRECH, R. (1985). *Acta Cryst.* B**41**, 21–26.

SIROTA, M. I. & MAKSIMOV, B. A. (1984). *Kristallografiya*, **29**, 34–38.

ZHANG, P. L., YAN, Q. W. & BOUCHERLE, J. X. (1988). *Acta Cryst.* C**44**, 592–595.

ZUCKER, U. H., PERENTHALER, E., KUHS, W. F., BACHMANN, R. & SCHULZ, H. (1983). *J. Appl. Cryst.* **16**, 358.

Acta Cryst. (1993). B**49**, 28–56

Structural Relations in Copper Oxysalt Minerals. I. Structural Hierarchy

BY RAY K. EBY* AND FRANK C. HAWTHORNE

Department of Geological Sciences, University of Manitoba, Winnipeg, Manitoba, Canada R3T 2N2

(*Received* 11 *September* 1990; *accepted* 2 *July* 1992)

Abstract

A hierarchical structural classification is developed for the copper oxysalt minerals, based on the polymerization of coordination polyhedra of higher bond valences, and focusing specifically on [3]-, [4]-, [5]- and [6]-coordinate polyhedra. The nature of copper oxysalt structures is complicated by the extremely distorted coordinations often occurring around the Cu^{2+} cation, a result of the well-known Jahn–Teller

* Present address: Department of Geology, University of Toronto, Toronto, Ontario, Canada M55 1A7.

0108-7681/93/010028-29$06.00